

# Biwindowed Discrete Multitone Transceiver Design

Bahram Borna and Timothy N. Davidson, *Member, IEEE*

**Abstract**—A family of biwindowed discrete multitone (DMT) transceivers that provide both subchannel spectral containment at the transmitter and spectral selectivity at the receiver is proposed. These systems have the attractive feature that they provide spectral shaping at both ends of the transceiver without requiring the cyclic prefix to be longer than the order of the channel impulse response. The windows are designed in a channel independent manner and are constrained to produce subchannel outputs that are free from (intrasubchannel) intersymbol interference (ISI). Furthermore, the design allows the intersubchannel interference (ICI) to be controlled in such a way that it can be mitigated using a relatively simple minimum mean-square error (MMSE) successive interference cancellation scheme. Under a realistic model for a digital subscriber line (DSL) environment, the achievable bit rate of the proposed system is significantly higher than that of the conventional DMT system and some established windowed DMT systems with receiver-only windowing. This performance gain is a result of the capability of the proposed system to combat the near-end crosstalk (NEXT) at the transmitter and receiver and to mitigate the narrowband noise at the receiver, without the requirement of excess cyclic prefix.

**Index Terms**—Discrete multitone (DMT), orthogonal-frequency-division multiplexing (OFDM), spectrum control, windowing.

## I. INTRODUCTION

MULTICARRIER communications systems have become popular due to their ability to efficiently communicate at high data rates over frequency-selective channels. Different classes of multicarrier techniques include discrete multitone (DMT), orthogonal-frequency-division multiplexing (OFDM), discrete wavelet multitone (DWMT), and filtered multitone (FMT) [1]–[4]. Among these, DMT and OFDM have attracted more attention, mainly due to their comparatively low complexity. However, the (implicit) pulse shaping and receive filters in the standard DMT and OFDM<sup>1</sup> systems are rectangular windows, and hence they suffer from rather poor frequency characteristics. The poor spectral containment at the transmitter can make it quite awkward to design schemes that are required to satisfy certain egress standards, such as those related to the amateur radio (HAM) bands in very high

speed digital subscriber line (VDSL) transceivers [1], [2]. This poor spectral containment also makes the system susceptible to performance loss caused by near-end crosstalk (NEXT). The poor spectral selectivity at the receiver makes the system susceptible to NEXT and to narrowband noise, such as radio frequency interference (RFI) emerging from AM broadcast and HAM radio signals. Therefore, there is the potential for significant performance gains if one can improve both the subchannel spectral containment at the transmitter and the spectral selectivity at the receiver.

Various schemes have been proposed to improve the spectral characteristics of DMT. These schemes involve different tradeoffs between the redundancy of the transmitted symbol stream, the complexity of the transmitter and receiver, and the amount of information about the channel (and the noise) that is required to synthesize the subchannels. The approach that will be proposed herein will have the same transmission redundancy as DMT, essentially the same transmitter complexity, and the synthesis of the subchannels will be independent of the channel (as in DMT). Consequently, there will be a moderate increase in the complexity of the receiver, but we feel that the performance gains offered by the proposed design make this a compelling tradeoff.

A convenient framework for comparing the proposed tradeoff with those (implicitly) chosen in some other schemes is that of the filter bank transceiver in Fig. 1, [3], [5]. (DMT is a special case of this framework.) For this system, the interference components of the subchannel outputs can be classified as being either intersubchannel interference (ICI), which arises from symbols transmitted on other subchannels, or (intrasubchannel) intersymbol interference (ISI), which arises from other symbols transmitted on the same subchannel. In the following discussion, we will focus on schemes in which the subchannels are synthesized in a channel-independent manner.

DMT operates on a block-by-block basis in the sense that the blocks of transmitted symbols generated by subchannel inputs at consecutive instants do not overlap. One approach to achieving better spectral properties than DMT is to allow the transmitter filters to be longer than  $N$ , and hence allow the transmitted blocks to overlap, e.g., DWMT [3] and FMT [4]. In DWMT, the subchannels are synthesized using a “critically sampled” perfect reconstruction or near-perfect reconstruction filter bank. This provides a considerable improvement in the spectral properties at both transmitter and receiver and the redundancy in the transmitted symbol stream is eliminated; i.e.,  $N = M$ . However, the lack of redundancy in DWMT makes it sensitive to channel distortion. Indeed, when the channel is frequency selective, the high levels of ISI and ICI require the use of complicated equalization and ICI cancellation schemes [6], [7]. In contrast to DWMT, the FMT scheme retains the redundant discrete Fourier transform (DFT) modulated filter bank structure of DMT. The prototype filter in the FMT filter bank can

Manuscript received April 26, 2006; revised October 31, 2006. The associate editor coordinating the review of this manuscript and approving it for publication was Dr. Luc Vandendorpe. This work was supported in part by the Natural Sciences and Engineering Research Council of Canada. The work of T. N. Davidson is also supported by the Canada Research Chairs program.

The authors are with the Department of Electrical and Computer Engineering, McMaster University, Hamilton, ON L8S 4K1, Canada (e-mail: borna@grads.ece.mcmaster.ca; davidson@mcmaster.ca).

Digital Object Identifier 10.1109/TSP.2007.895992

<sup>1</sup>For simplicity, we will use the term DMT for the systems of interest, but the proposed designs apply equally well to OFDM.

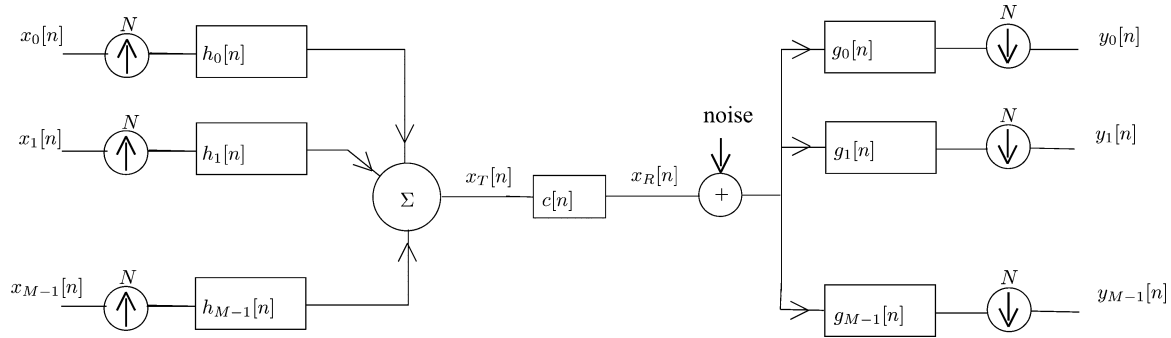


Fig. 1.  $M$ -subchannel filter bank communication system.

be designed in a channel-independent manner to provide excellent spectral properties and negligible ICI [4], [8]. However, the FMT prototype filter is usually quite long—often of the order of ten times the number of subchannels—which increases the complexity of the transceiver. Furthermore, in order to achieve negligible ICI, some residual ISI is incurred, and hence significant per-subchannel equalization is required [4], [8], [9].

While FMT provides subchannels with desirable spectral properties and systems with large achievable rates, its implementation is significantly more complex than that of DMT. Therefore, multicarrier communication systems with a complexity comparable to that of DMT, but with improved spectral characteristics are of significant interest. The so-called “windowed DMT” schemes represent a category of such systems. Like FMT, these schemes can be viewed as redundant DFT modulated filter bank transceivers, but they typically have a shorter prototype filter. This “window” is often short enough to preserve the block-by-block transmission characteristic of DMT. Some of the proposed windowed DMT schemes involve windowing at the transmitter to reduce the out of band energy of the transmitter subchannel signals [10]–[13], while others involve windowing at the receiver to improve the robustness of the transmission scheme to narrowband interference [14]–[16]. (An interesting channel-dependent receiver windowing approach appears in [17].) In most of these techniques, the design is contingent on the cyclic prefix being longer than the channel order in order to avoid window-induced ISI and ICI. Unfortunately, this requirement reduces the spectral efficiency of the transmitted symbol stream. There has been some progress in the design of transmitter or receiver windowed DMT schemes without the requirement of excess cyclic prefix [10], [13], but these schemes only operate at one end of the transceiver, and additional processing in the form of equalization and ICI cancellation is required at the receiver.

A shortcoming of the existing channel-independent windowing methods is that they require excess redundancy in the form of a cyclic prefix that must be longer than the order of the channel, and/or they are designed to improve the subchannel spectrum only at one end of the transceiver. In this paper, we propose a channel-independent windowing method that improves both the subchannel spectral containment at the transmitter and the subchannel spectral selectivity at the receiver, without the requirement of excess redundancy. Since improved subchannel spectra are obtained at both ends of the

transceiver, the egress standards are easier to meet, NEXT is reduced, and mitigation of narrowband noise is improved. As we will show in our simulations, the reduction of NEXT, the mitigation of narrowband noise, and the absence of a requirement for excess cyclic prefix can result in a significant gain in the achievable bit rate. The proposed biwindowed DMT system preserves many of the desirable features of DMT. In particular, block-by-block transmission is maintained at the same level of redundancy, the subchannel outputs are free from ISI, no knowledge of the channel is required in the design of the windows, and a closed-form expression for the designed window can be obtained. In order to achieve the desired spectral shaping while preserving these features, some ICI is allowed, but the ICI is controlled in such a way that it can be mitigated using a relatively simple minimum mean-square error (MMSE) successive interference cancellation scheme. While this interference canceller does increase the receiver complexity to some degree, our numerical results suggest that in a realistic digital subscriber line (DSL) environment, the proposed scheme provides a significant increase in the achievable rate over that of standard DMT.

This paper is organized as follows: In Section II, the system is analyzed, and the channel-independent ISI-free conditions are stated. The proposed window design is presented in Section III, and Section IV contains the description of the MMSE successive ICI canceller. In Section V, we provide simulation results which illustrate the performance achieved by the proposed system in a realistic DSL environment. Concluding remarks are provided in Section VI.

## II. SYSTEM ANALYSIS

In order to facilitate comparisons to a broad range of multicarrier systems, we will develop our windowed transceiver within the framework of the filter bank transceiver in Fig. 1. DMT and OFDM are special cases of this framework in which  $N = M + P$ , where  $P$  is the length of the cyclic prefix, and the transmit and receive filters are obtained by DFT modulation (of fundamental frequency  $2\pi/M$ ) of rectangular windows of lengths  $N$  and  $M$ , respectively. We will denote the impulse response of the equivalent discrete-time channel (including any time domain equalization) by  $c[n]$ , and it will be assumed that  $c[n]$  can be nonzero only for  $0 \leq n \leq L$ . The additive noise in Fig. 1 represents all external noise and interferences, including

additive white Gaussian noise (AWGN), radio frequency interference (RFI), and crosstalk. The output of the  $m$ th subchannel of the receiver in Fig. 1 can be written as (e.g., [3])

$$y_m[n] = \sum_k g_m[k] \sum_{p=0}^L c[p] \sum_{i=0}^{M-1} \sum_{\ell} x_i[\ell] \times h_i[N(n-\ell) - k - p] + v_m[n] \quad (1)$$

$$= \sum_{i=0}^M \sum_k x_i[n-k] c_{mi}[Nk] + v_m[n] \quad (2)$$

where

$$c_{mi}[n] = h_i[n] \star c[n] \star g_m[n], \quad (3)$$

the symbol  $\star$  denotes the convolution operator, and  $v_m[n]$  represents the (zero-mean) additive noise of Fig. 1 after being filtered by  $g_m[n]$  and downsampled by a factor of  $N$ . If  $k_0$  denotes the synchronization delay of the system, then the term  $\sum_{k \neq k_0} x_i[n-k] c_{mm}[Nk]$  in (2) is the ISI on subchannel  $m$ , and  $\sum_{i \neq m} \sum_k x_i[n-k] c_{mi}[Nk]$  is the ICI.

The first goal of our design is to preserve the property of standard DMT systems that the subchannel outputs are free from ISI for all channels  $c[n]$  of order at most  $L$ , as long as the order of channel is not longer than the cyclic prefix length, i.e.,  $L \leq P$ . In Appendix I, we have derived necessary and sufficient conditions for this property to hold. A desirable special case of those conditions is

$$h_i[n] = 0, \quad n \notin [0, N-1] \quad (4)$$

$$g_m[k] = 0, \quad k \notin [1, N-L] \quad (5)$$

and we will assume that (4) and (5) hold in the rest of the paper. Conditions (4) and (5) also hold for standard DMT and in the windowed DMT systems based on Nyquist windowing [14]–[16].

Substituting (4) and (5) into (2), we have that

$$y_m[n] = \sum_{i=0}^{M-1} x_i[n-1] c_{mi}[N] + v_m[n] \quad (6)$$

from which it is clear that the subchannel outputs are free from ISI. However, it is also clear that  $y_m[n]$  is not free from ICI. Indeed, the output of each subchannel at instant  $n$  is, in general, a weighted sum of all subchannel inputs at instant  $n-1$ . (It does not depend on the subchannel inputs at other instants.) In order to simplify the analysis of the ICI of the system, we define

$$f_{mi}[n] = h_i[n] \star g_m[n] \quad (7)$$

and rewrite the ICI coefficients in (3) as

$$c_{mi}[N] = \sum_{k=0}^L c[k] f_{mi}[N-k]. \quad (8)$$

This expression makes it clear that if we wish to ensure that the ICI coefficients  $c_{mi}[N]$ ,  $i \neq m$ , are small for any channel of order at most  $L$ , we must ensure that coefficients  $f_{mi}[n]$  are small for all  $N-L \leq n \leq N$  and  $i \neq m$ . Moreover, the

channel-independent zero ICI condition reduces to  $f_{mi}[n] = 0$  for all  $i \neq m$  and  $N-L \leq n \leq N$ .

### III. WINDOW DESIGN

Having established the conditions for an ISI-free filter bank transceiver, we now develop a channel-independent design method for the transmitter and receiver windows. The goal is to obtain both a high level of subchannel spectral containment at the transmitter and a high level of spectral selectivity at the receiver, while limiting the impact of ICI. The windowed DMT system is embedded in the filter bank model in Fig. 1 and is exposed when the filter bank has the following DFT modulated structure:

$$h_i[n] = h[n] e^{j \frac{2\pi}{M} in} \quad (9)$$

$$g_m[n] = g[n] e^{j \frac{2\pi}{M} nm} \quad (10)$$

where  $h[n]$  and  $g[n]$  are the transmit and receive windows, respectively. In that case, the term  $f_{mi}[n]$  in (7) can be written as

$$f_{mi}[n] = e^{j \frac{2\pi}{M} nm} \sum_{k=0}^{N-1} h[k] g[n-k] e^{j \frac{2\pi}{M} k(i-m)}. \quad (11)$$

In the case that  $L = P$ , (i.e.,  $N = M + L$ ), and  $h[\cdot]$  and  $g[\cdot]$  are rectangular windows supported on the intervals in (4) and (5), respectively, we have a standard DMT system.<sup>2</sup> In that case, it can be verified that  $f_{mi}[n] = 0$  for all  $N-L \leq n \leq N$  and all  $i \neq m$ . Hence,  $c_{mi}[N] = 0$  for all  $i \neq m$ , and there is no ICI at the receiver. When the cyclic prefix is longer than is required for the given channel (i.e., when  $P > L$ ), the excess redundancy in the transmitted signal can be exploited to design systems with zero ICI and a spectral shaping window at the receiver (e.g., the receiver Nyquist windowing in [14]–[16]), or a spectral shaping window at the transmitter (e.g., [11] and [12]). The goal of the present paper is to design systems with spectral shaping windows at both the transmitter and receiver, without requiring the cyclic prefix to be longer than the order of the channel.

Seeing as the goal for our window design is to improve the spectral properties of the system without requiring excess redundancy, we will set the length of the cyclic prefix to be equal to the order of the channel, i.e.,  $P = L$ . We will ensure that the subchannel outputs are free from ISI by constraining  $h[\cdot]$  and  $g[\cdot]$  to comply with (4) and (5), respectively. Our design strategy is to seek a pragmatic channel-independent design procedure, and to show (in Section V) that this procedure provides substantial performance improvement. We will adopt a sequential design procedure<sup>3</sup> in which we first design a receiver window,  $g[\cdot]$ , supported on the interval in (5) with desirable spectral characteristics, i.e., with small stopband energy and rapid spectral

<sup>2</sup>In systems in which the actual length of the channel is not known (e.g., wireless OFDM systems), the appropriate statement is  $L_{\max} = P$ , where  $L_{\max}$  is the order of the longest channel that is postulated in the design.

<sup>3</sup>Although a joint design procedure can be conceived,  $f_{mi}[n]$  in (11) is a bilinear function of the windows, and hence the formulation of joint design problems is usually nonconvex. As a result, joint design procedures may require careful management of locally optimal solutions in order to obtain a solution that is sufficiently close to a global optimum.

roll-off. This can be done using standard window design techniques, such as those in [18], [19]. We will then design the transmitter window in a way that balances the objectives of transmit subchannel spectral containment and ICI suppression. The design procedure begins with the design of the receiver window because the receiver must mitigate both NEXT and narrowband noise.

In the design of the transmitter window, we will measure spectral containment using the energy in the stopband of the window, and we will measure ICI suppression using the sum of the squares of  $f_{mi}[n]$  in (11) for  $N - L \leq n \leq N$ . Therefore, a natural formulation of the design problem is

$$\begin{aligned} \text{minimize } & \frac{\lambda}{2\pi} \int_{\theta}^{2\pi-\theta} |H(e^{j\omega})|^2 d\omega \\ & + (1-\lambda) \sum_{p=1}^{M-1} \sum_{n=N-L}^N \left| \sum_{k=0}^{N-1} h[k]g[n-k]e^{j\frac{2\pi}{M}kp} \right|^2 \end{aligned} \quad (12a)$$

$$\text{subject to } \sum_{n=0}^{N-1} h[n] = 1 \quad (12b)$$

where  $H(e^{j\omega})$  denotes the Fourier transform of  $h[n]$ ,  $\theta$  is a constant that defines the stopband for  $H(e^{j\omega})$  as  $[\theta, 2\pi - \theta]$ , and  $\lambda \in [0, 1]$  weights the objectives of spectral containment and ICI suppression. The constraint in (12b) fixes the dc gain of the transmitter window  $H(e^{j0})$  to one. The optimization problem in (12) is a (strictly) convex quadratic program with a single linear equality constraint, and hence a closed-form solution can be easily obtained using the classical Lagrange multiplier method [21]; the details are provided in Appendix II.<sup>4</sup>

It is clear from the formulation in (12) that the parameter  $\lambda$  allows the designer to adjust the relative importance of ICI suppression and spectral containment in the design of the window. Although  $\lambda$  provides some control over the level of ICI, our goal of improving the spectral containment at the transmitter over that of the conventional DMT scheme while retaining a cyclic prefix length that is equal to (not greater than) the order of the channel means that ICI is inevitable. In order to mitigate the effect of the residual ICI, we propose the use of MMSE successive ICI cancellers.

#### IV. ICI CANCELLATION

The behavior of the ICI of the proposed system is captured by the ICI coefficients  $c_{mi}[N]$  [c.f., (6)]. Since we have a DFT modulated filter bank [c.f., (9) and (10)], the frequency-domain counterpart to (3) can be written as

$$C_{mi}(e^{j\omega}) = H\left(e^{j(\omega-2\pi i/M)}\right) C(e^{j\omega}) G\left(e^{j(\omega-2\pi m/M)}\right) \quad (13)$$

<sup>4</sup>An alternative to (12b) is energy normalization  $\sum_n |h[n]|^2 = 1$ . The closed-form solution of that problem is also well known (e.g., [22]) and is the eigenvector that corresponds to the minimum eigenvalue of the matrix  $\Psi$  given by (27) in Appendix II. In the design examples in Section V, the spectrum of the optimal window for the dc constraint of (12b) and that of the optimal window for the energy constraint are indistinguishable.

where  $X(e^{j\omega})$  denotes the Fourier transform of  $x[\cdot]$ . Since  $g[\cdot]$  is chosen so that  $G(e^{j\omega})$  has a small stopband energy, and  $h[\cdot]$  is designed using (12), which ensures a small stopband energy for  $H(e^{j\omega})$ , one can see from (13) that  $C_{mi}(e^{j\omega})$  will have non-negligible values only if  $|m-i|$  is close to zero or close to  $M$ . In order to suppress the non-negligible ICI terms at the subchannel outputs, we propose the use of MMSE successive ICI cancellers. Since the output of each subchannel at instant  $n$  depends on subchannel inputs at instant  $n-1$ , but not on subchannel inputs at other instants, we will simplify our notation by dropping the time arguments  $n$  and  $n-1$  in (6) and rewriting it as

$$y_m = \sum_{i=0}^{M-1} x_i \tilde{c}(m, i) + v_m \quad (14)$$

where  $\tilde{c}(m, i) = c_{mi}[N]$ . Since only a few of the  $M-1$  ICI terms in (14) will have non-negligible values, we will only take those non-negligible values into account in the design of the ICI cancellers. In other words, we will assume that

$$y_m \approx \sum_{i=m\oplus\nu}^{m\ominus\nu} x_i \tilde{c}(m, i) + v_m \quad (15)$$

where it has been assumed that  $2\nu$  ICI terms have non-negligible values, and  $\oplus$  and  $\ominus$  represent the modulo- $M$  addition and subtraction operators, respectively.

To detect  $x_m$  from  $y_m$ , we employ an MMSE successive ICI canceller with  $K_1+1$  "feedforward" coefficients, and  $K_2$  "feedback" coefficients. (These terms are borrowed from the terminology of decision feedback equalization.) A block diagram of such an ICI canceller is shown in Fig. 2, where the input to the symbol detector is

$$\hat{x}_m = \sum_{k=-K_1+\nu}^{\nu} a_k y_{m\oplus k} + \sum_{k=1}^{K_2} b_k \tilde{x}_{m\oplus k} \quad (16)$$

and  $\tilde{x}_k$  denotes the decision made on the symbol in subchannel  $k$ . An interesting feature of this scheme is that it operates within each block of the received symbols, and independently of other blocks [c.f., (14)]. To compute the feedforward and feedback coefficients of the ICI canceller, we make the standard assumption that in the system of Fig. 1 the input data sequences of different subchannels are uncorrelated, and we will denote the power of the  $i$ th input sequence  $x_i[\cdot]$  by  $P_i$ . By applying the orthogonality principle [23] for MMSE estimation, it can be shown that the feedforward coefficients can be obtained from the following set of linear equations:

$$\sum_{n=-K_1+\nu}^{\nu} a_n \psi_{jn} = P_m \tilde{c}^*(m \ominus j, m), \quad j = -K_1 + \nu, \dots, \nu - 1, \nu \quad (17)$$

where

$$\begin{aligned} \psi_{jn} = & \sum_{r=-\nu}^{-j} \tilde{c}^*(m \ominus j, m-j-r) \tilde{c}(m \ominus n, m-j-r) P_{m\oplus j\oplus r} \\ & + R_v(m \ominus n, m \ominus j), \quad j, n = -K_1 + \nu, \dots, \nu - 1, \nu \end{aligned} \quad (18)$$

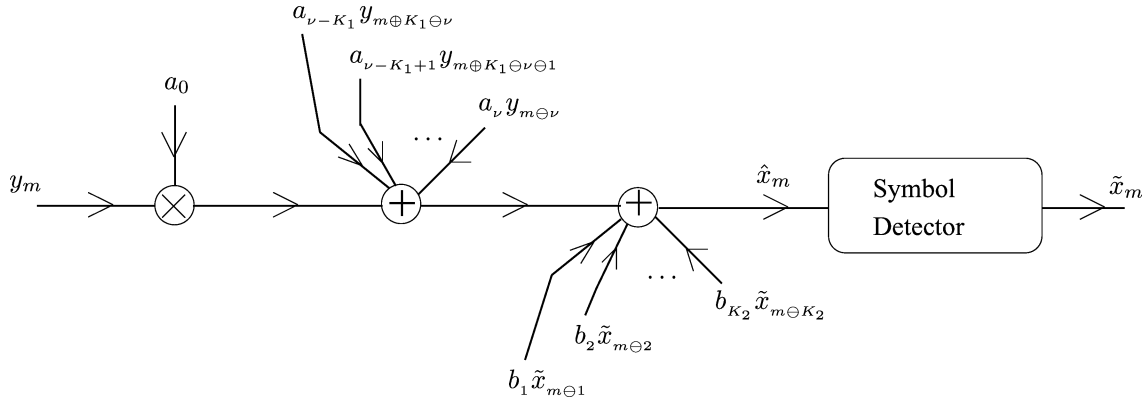


Fig. 2. Successive ICI canceller with decision feedback.

and  $R_v(k, \ell) = E\{v_k v_\ell^*\}$  is the noise covariance at the subchannel outputs. The feedback coefficients are given by

$$b_\ell = - \sum_{j=-K_1+\nu}^{\nu} a_j \tilde{c}(m \ominus j, m \ominus \ell), \quad \ell = 1, 2, \dots, K_2. \quad (19)$$

In Section V, examples of the proposed biwindowed DMT system are presented for a realistic DSL environment, and we will see that for values of  $\nu$ ,  $K_1$ , and  $K_2$  as small as 3, 6, and 6, respectively, significant performance gains can be achieved. Being able to obtain a high level of subchannel spectral containment at the transmitter and a high level of subchannel spectral selectivity at the receiver with such small values of  $\nu$ ,  $K_1$ , and  $K_2$  is an attractive feature of the proposed system.

Recall from (16) that for the detection of the symbol transmitted on a given subchannel, the previously detected symbols on  $K_2$  subchannels are used. Thus, for each block of the received signal, the process of detection and successive ICI cancellation requires a starting point. If we assume that this process starts from the  $j$ th subchannel, the symbols that are sent through subchannels  $j \ominus 1, j \ominus 2, \dots, j \ominus K_2$  have to be known symbols for the receiver. In other words, among the  $M$  subchannels of the system, the symbols transmitted on a contiguous set of  $K_2$  of them are assumed to be known at the start of the detection and ICI cancellation procedure. Fortunately, most DMT systems use digital duplexing [2], in which the upstream and downstream frequency bands are specified by dividing the  $M$  subchannels into a number of groups, each representing an upstream or downstream band. A typical example of such subchannel grouping into downstream and upstream bands is given in Section V (see Fig. 6). In such scenarios, the detection for the subchannels of each downstream or upstream frequency band can be performed independently of the other bands. Moreover, in each frequency band, one can choose to start the detection procedure at the lower edge of the band. In this case, the  $K_2$  subchannels that lie below the subcarrier on the lower edge of the band belong to a band that is assigned to the opposite direction of communication. Therefore, the corresponding symbol values in the current direction can be set to zero, and hence, it

will not be necessary to restrict  $K_2$  subchannels to carry known symbols.

## V. NUMERICAL RESULTS

In this section, we will provide examples of the subchannel spectra that can be achieved by the proposed system, and will provide a numerical comparison of the achievable rates of the proposed system and those of receiver-only Nyquist windowed DMT schemes [14], [15] in a realistic model for a DSL environment. We consider windowed DMT systems with  $M = 512$  conjugate symmetric subchannels and a cyclic prefix of length  $P = 40$ , i.e.,  $N = 552$ . These values represent one set of valid values for  $M$ ,  $P$ , and  $N$  adopted in the VDSL2 standard [2].

Recall from Section III that in the proposed method, the receiver window is designed using existing techniques or is chosen from the set of standard windows, and we design the transmitter window using the optimization problem in (12), for which the closed-form solution is provided in Appendix II. Among the standard windows [18]–[20], the Hann and Blackman windows have small stopband energies and a rapid spectral roll-off, and hence we chose the Hann and Blackman windows as the candidate receiver windows for the proposed system.

In the examples that we will present for the biwindowed system, we assume that the shortest admissible cyclic prefix is used. Therefore, we assume that the channel (if not already short enough) is shortened using a time-domain equalizer (TEQ) [24]–[26] to length  $L + 1 = P + 1 = 41$ . Hence, the receiver window will be of length  $N - L = 512$  [c.f., (5)]. The receiver-only Nyquist windowing schemes [14], [15] require extra redundancy, and for those schemes, we will use a TEQ with a shorter target impulse response length.

In our first design, we chose the receiver window,  $g[\cdot]$ , to be a Hann window [19] of length 512, and we designed the transmitter window  $h_1[\cdot]$  of length  $N = 552$  using the closed-form solution for the optimization problem in (12) with the parameters  $\lambda = 0.5$  and  $\theta = 4\pi/M$ . The power spectrum of the designed transmitter window is shown in Fig. 3, along with the power spectrum of a length- $N$  rectangular window, which is the (implicit) transmitter window of the conventional DMT system. Similarly, we designed the transmitter window  $h_2[\cdot]$  of length 552 for the case in which the receiver window is the Blackman window [19] of length 512, using the same values of

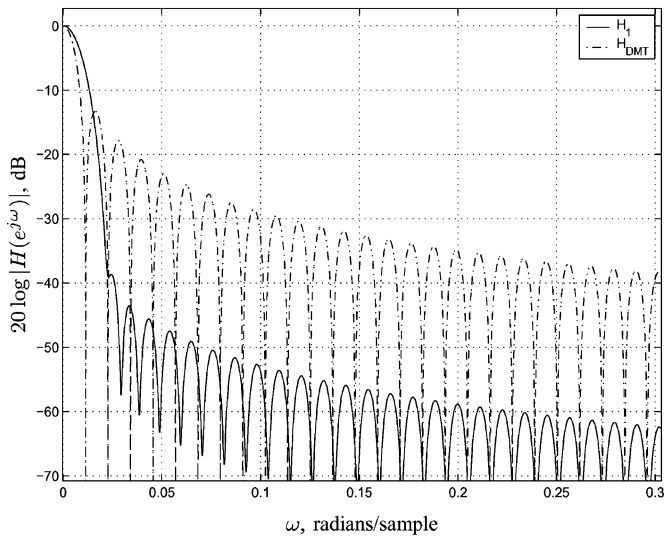


Fig. 3. Frequency response of the designed transmitter window of length  $N = 552$  (solid line) when the receiver window is a Hann window of length  $M = 512$ ,  $\lambda = 0.5$ , and  $\theta = 4\pi/M$ . The dashed curve is the frequency response of the rectangular window of length  $N = 552$ .

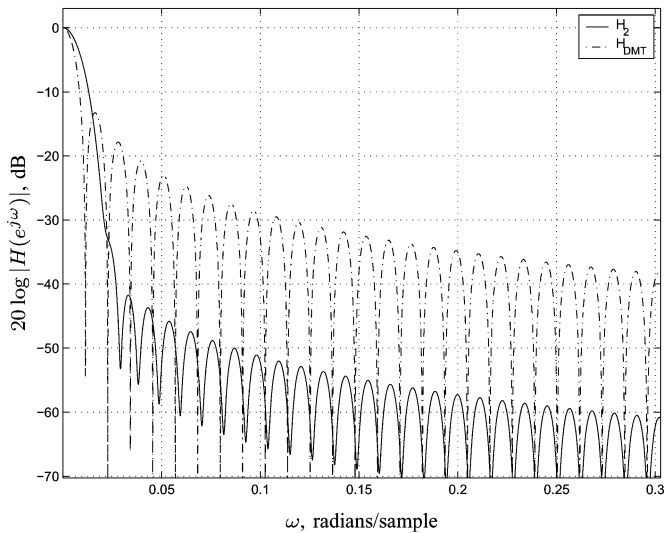


Fig. 4. Frequency response of the transmitter window of length  $N = 552$  (solid line) when the receiver window is a Blackman window of length  $M = 512$ ,  $\lambda = 0.5$ , and  $\theta = 4\pi/M$ . The dashed curve is the frequency response of the rectangular window of length  $N = 552$ .

$\lambda$  and  $\theta$ . The power spectrum of that window is shown in Fig. 4. Fig. 5 shows the time-domain shapes of the designed transmitter windows.

In order to illustrate the performance improvement that can be achieved by the proposed transceiver, we will evaluate various system characteristics in a realistic model for a DSL environment. The voice-grade unshielded twisted pair cable (UTP-3) model [4] was used as the channel model, and an MMSE-TEQ [24]–[26] was used to shorten this physical channel to a given target length. NEXT and far-end crosstalk (FEXT) were simulated using the model for a 50-pair binder [1]. Symmetric transmission with a sampling rate of  $1/T_s = 2.208$  Msamples/s was implemented using digital duplexing [2] with the spectrum plan

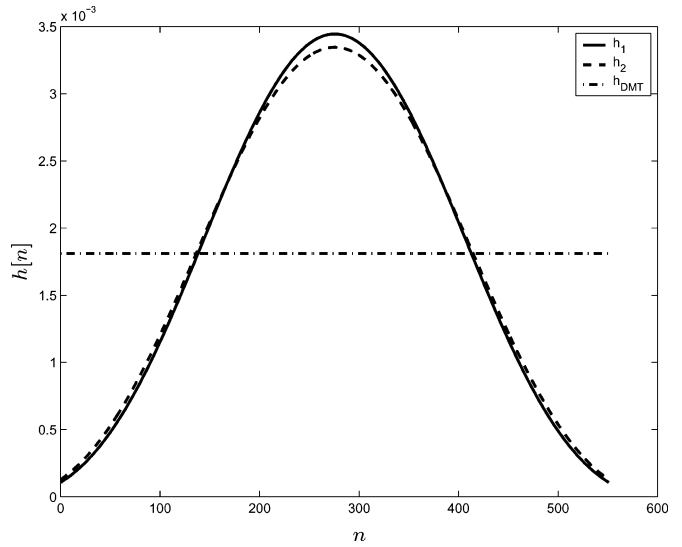


Fig. 5. Time-domain shapes (interpolated) of the designed transmitter windows for the proposed system. For comparison, the rectangular transmitter window of the conventional DMT system is also plotted.

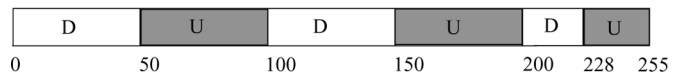


Fig. 6. Spectrum plan used in the simulations. Subchannels 0–49, 100–149, and 200–227 are assigned for downstream communication (marked by “D”), and the remaining subchannels are used for upstream (U) transmission.

TABLE I  
MODEL 1 RADIO NOISE OF [27] FOR AM RADIO SIGNALS FOR  
FREQUENCIES BELOW 1.104 MHz

Frequency (kHz)	Differential mode power (dBm)
660	-60
710	-30
770	-70
1050	-55

shown in Fig. 6. The transmit signal power was 10 dBm, the AWGN power spectral density was  $-140$  dBm/Hz, and it was assumed that echo was perfectly cancelled. Model 1 radio noise from [1] and [27] was used for the simulation of the RFI caused by the AM radio signals. Only the four of the ten AM signals of that model that lie below 1.104 MHz were used. Table I lists the frequency and power for these RFI signals.

Our first investigation concerns the ICI characteristics of the proposed system. In order to visualize the localized nature of the significant ICI components, in Fig. 7, we have depicted the normalized magnitudes of the ICI coefficients  $\check{c}(m, i)$  for three representative subchannels:  $m = 20, 60$ , and  $100$ . This figure is for the case of the first design (c.f., Fig. 3), and the length of the cable is 2000 m. If we deem an ICI component to be negligible if its power is at least 60 dB below the power of the desired component, then it can be seen from Fig. 7 that for each of the illustrated subcarriers, the number of non-negligible ICI terms is 6. In fact, this holds true for all subcarriers in both example designs of the proposed system. Therefore, in the implementation of the ICI cancellers, we chose  $\nu = 3$  in (15), and hence

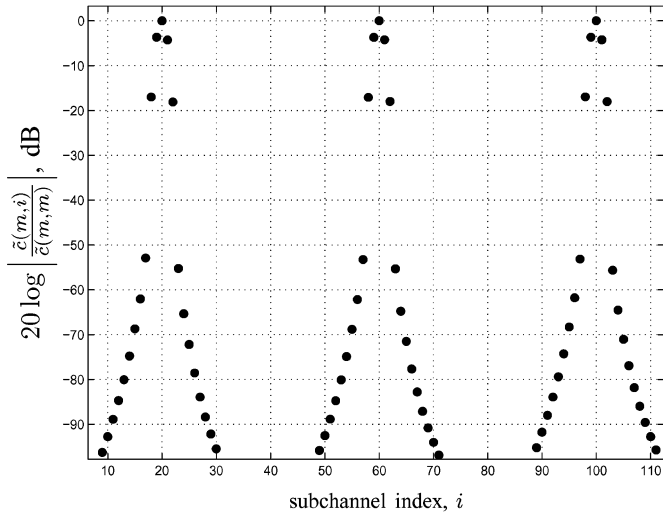


Fig. 7. Normalized ICI factors corresponding to subchannels  $m = 20, 60$  and  $100$  (see (14)).

the number of coefficients for the feedforward and feedback sections of the MMSE successive ICI cancellers at the subchannel outputs were chosen to be 7 and 6, respectively.

Our second performance evaluation is that of the achievable bit rate for the downstream communication. This was evaluated using the standard expression (e.g., [1]):

$$R = \frac{1}{T} \sum_{i \in \mathcal{A}} \log_2 \left( 1 + \frac{\text{SINR}_i \gamma_{\text{code}}}{\Gamma \gamma_{\text{margin}}} \right) \quad (20)$$

where  $\text{SINR}_i$  is the signal-to-noise-plus-interference ratio of the  $i$ th subchannel at the input to the symbol detector in the ICI canceller, and  $\Gamma$  denotes the SINR gap, which for QAM modulation at a bit error probability of  $10^{-7}$  is 9.8 dB, [1]. The parameter  $\gamma_{\text{code}}$  is the coding gain, which is assumed to be 3 dB, and  $\gamma_{\text{margin}}$  is the additional SINR margin, which, in the absence of error propagation, is chosen to be 3 dB. For the two examples of the proposed system, our simulation studies show that, at a bit error probability of  $10^{-7}$ , error propagation can result in a maximum SNR loss of 0.52 dB. Thus, for the two examples of the proposed system, we will choose an SNR margin of  $3 + 0.52 = 3.52$  dB. In (20),  $\mathcal{A}$  denotes the set of downstream subchannel indices, and  $1/T = 1/(NT_s) = 4$  kHz is the symbol rate. The SINR of each downstream subchannel of the proposed system was obtained by simulation in the above-mentioned DSL environment, and the achievable rate was computed using (20) with  $\gamma_{\text{margin}} = 3.52$  dB. The achievable rates of the two examples of the proposed system are plotted against the cable length in Fig. 8. In order to indicate the improvement that can be obtained by the proposed system, we also provide in Fig. 8 the achievable bit rates for the standard DMT system, and for the Nyquist receiver-only windowed DMT systems with a piecewise constant window [15], and a raised cosine window [14], [15]. (Notice that for these schemes,  $\gamma_{\text{margin}} = 3$  dB.) These Nyquist receiver-only windowing schemes require excess redundancy. We considered an excess redundancy of length  $\mu = 10$ , and we realized this excess redundancy by setting the target length for the TEQ-shortened channel to  $P + 1 - \mu = 31$ . (For the proposed bi-windowed system, the TEQ need only shorten the channel to

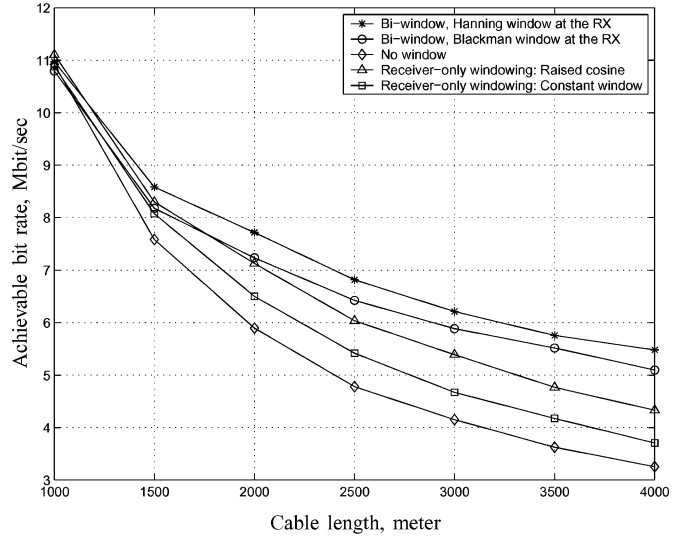


Fig. 8. Achievable bit rate versus the cable length for the downstream communication.

a length of  $L = 41$ .)<sup>5</sup> From the comparisons in Fig. 8, it can be seen that the proposed biwindowed DMT system provides a considerably higher achievable rate than the receiver-only windowing schemes for all the considered cable lengths, with the proposed system that employs the Hann window at the receiver providing a slightly higher rate than that based on the Blackman window. Fig. 8 also suggests that the achievable rate gain obtained by the proposed system is more significant for longer cables.

The increased achievable rates obtained by the proposed system are a consequence of two mechanisms. First, in addition to the mitigation of the narrowband noise and the NEXT by the receiver window, NEXT is also mitigated by the transmitter due to the small stopband energy of the transmitter window. Second, in the proposed system, the receiver window is not constrained to satisfy the time-domain Nyquist condition [14], [15], and hence windows with smaller sidelobes and smaller stopband energy can be obtained. In order to illustrate the ability of the proposed system to suppress NEXT and narrowband noise, we have plotted in Figs. 9 and 10, respectively, the NEXT-to-signal and RFI-to-signal power ratios at the receiver outputs of three systems for downstream transmission over a cable of length of 2000 m. (Recall the downstream bands from the spectrum plan in Fig. 6.) The three systems are the proposed biwindowed DMT system with Hann window at the receiver, a receiver-only windowed DMT system with a raised cosine window, and the standard DMT system with its rectangular windows. From Fig. 9, it can be seen that the biwindowed DMT system provides much stronger suppression of NEXT interference due to the fact that it uses windowing at both the transmitter and the receiver. Fig. 10 shows that the proposed system also provides stronger suppression of narrowband interference than the receiver-only windowing approach with

<sup>5</sup>We used an MMSE-TEQ [25] with 15 taps for the target impulse response (TIR) of length 41 and an MMSE-TEQ with 20 taps for the TIR of length 31. This choice was made in order to obtain similar values for the residual mean square error. Moreover, the synchronization delay for each of the TEQs was optimized by numerical search.

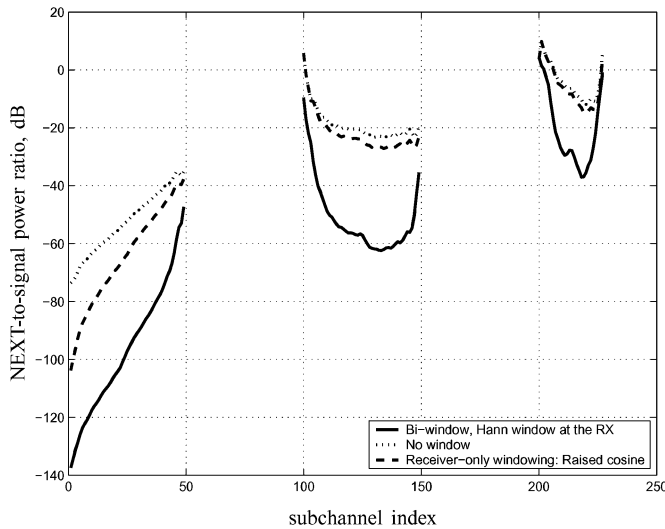


Fig. 9. NEXT-to-signal power ratios at the subchannel outputs (interpolated) for the downstream transmission bands, with a cable length of 2000 m.

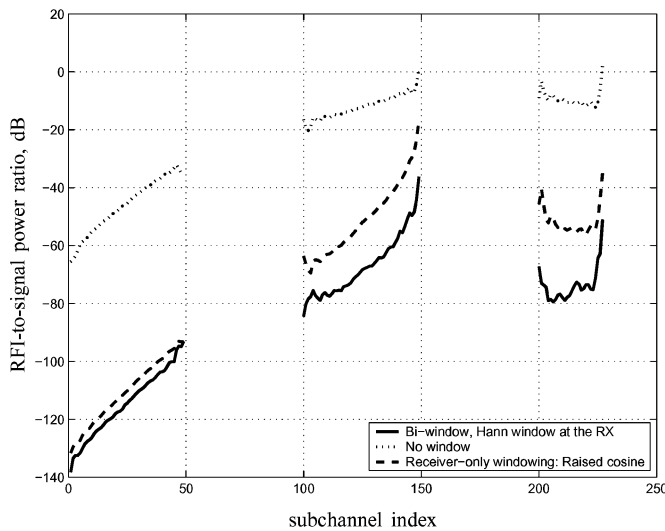


Fig. 10. RFI-to-signal power ratios at the subchannel outputs (interpolated) for the downstream transmission bands, with a cable length of 2000 m.

a raised cosine window. As mentioned earlier, this is because, in the proposed system, the receiver window is not constrained to satisfy the time-domain Nyquist condition [14], [15], and therefore receiver windows with smaller sidelobes and smaller stopband energy can be used.

## VI. CONCLUSION

We have proposed a family of biwindowed DMT systems that provides improved subchannel spectral characteristics at both ends of the transceiver without the requirement of excess cyclic prefix. Compared to the standard DMT system and to windowed DMT systems with receiver-only (Nyquist) windowing, the proposed system provides a considerable gain in the achievable bit rate in the presence of narrowband noise and crosstalk. The proposed design does not require the knowledge of the channel, other than the assumption that the order of the shortened equivalent discrete-time channel is not larger than the cyclic prefix

length. In the proposed transceiver, the received signal in each subchannel is free from ISI and has only a small number of non-negligible ICI components. Successive ICI cancellers were proposed to suppress the non-negligible ICI terms that exist at the subchannel outputs. Numerical results demonstrated the capability of the proposed system to provide a significant increase in the achievable bit rate in a realistic DSL environment.

## APPENDIX I DERIVATION OF THE CHANNEL-INDEPENDENT ZERO ISI CONDITIONS

In this appendix, we derive the necessary and sufficient condition for the filter bank transceiver of Fig. 1 to be free from ISI for all channels of order at most  $L$ . Assume that the transmit filters  $h_i[\cdot]$  are supported on  $[n_1, n_2]$  and that the receive filters  $g_m[\cdot]$  are supported on  $[k_1, k_2]$ . In order for the subchannel outputs to be free from ISI,  $y_m[n]$  in (1) should depend on  $x_m[\ell]$  for one, and only one, instant  $\ell$ . Given the support intervals of  $h_i[\cdot]$ ,  $c[\cdot]$  and  $g_m[\cdot]$ , this holds if and only if there is one, and only one, integer  $\ell$  that satisfies

$$k_1 + n_1 \leq N\tilde{\ell} \leq k_2 + n_2 + L. \quad (21)$$

If  $k_1 + n_1 = jN$  for some integer  $j$ , then  $\tilde{\ell} = j$  satisfies (21), and in order to prevent any  $\tilde{\ell} \geq j + 1$  from satisfying (21), one must ensure that  $k_2 + n_2 + L < (j + 1)N$ . If  $k_1 + n_1 = Nj + d$ , for some integer  $j$  and an integer  $d \in [1, N - 1]$ , then in order to ensure that one and only one value of  $\tilde{\ell}$  satisfies (21), one must ensure that  $N(j + 1) \leq k_2 + n_2 + L$  and  $N(j + 2) > k_2 + n_2 + L$ . By simplifying these expressions, we obtain the following necessary and sufficient condition for the system to be free from ISI for any channel of order at most  $L$ :

$$(k_2 - k_1) + (n_2 - n_1) < N - L, \quad \text{if } k_1 + n_1 = jN \quad (22a)$$

$$N - L \leq (k_2 - k_1) + (n_2 - n_1) + d < 2N - L, \quad \text{if } k_1 + n_1 = jN + d. \quad (22b)$$

In order to maximize the length of the allowable filters, we will impose (22b) in our design, with  $d = 1$ . We can choose the pair  $(n_1, j) = (0, 0)$  without loss of generality, and hence  $k_1 = 1$ . In order to involve all the coefficients of the transmitter filters in the spectral shaping of the transmitted subchannel signals, and, at the same time, ensure that all the coefficients of the receiver subchannel filters are used in the filtering of the received signal, we choose  $k_2 = N - L - n_1$ , and  $n_2 = N - k_1$ , and hence obtain (4) and (5).

## APPENDIX II CLOSED-FORM SOLUTION FOR THE OPTIMIZATION PROBLEM (12)

A closed-form solution to (12) can be obtained using the classical Lagrange multiplier method [21]. Let  $\mathbf{h}$  denote the  $N \times 1$  vector  $\mathbf{h} = (h[0], h[1], \dots, h[N - 1])^T$ , and let  $\mathbf{d}$  denote the  $N \times 1$  vector  $\mathbf{d} = (1, 1, \dots, 1)^T$ . The constraint (12b) can



then be written as  $\mathbf{d}^T \mathbf{h} = 1$ . Using the fact that  $H(e^{j\omega}) = \sum_{k=0}^{N-1} h[k]e^{-j\omega k}$ , we can write

$$\frac{1}{2\pi} \int_{\theta}^{2\pi-\theta} |H(e^{j\omega})|^2 d\omega = \mathbf{h}^T \mathbf{U} \mathbf{h} \quad (23)$$

where  $\mathbf{U}$  is an  $N \times N$  matrix with entries

$$[\mathbf{U}]_{\ell,k} = \begin{cases} 1 - \frac{\theta}{\pi}, & \ell = k \\ -\frac{\sin((k-\ell)\theta)}{(k-\ell)\pi}, & \ell \neq k. \end{cases} \quad (24)$$

We can also write

$$\sum_{p=1}^{M-1} \sum_{n=N-L}^N \left| \sum_{k=0}^{N-1} h[k]g[n-k]e^{j\frac{2\pi}{M}kp} \right|^2 = \mathbf{h}^T \mathbf{V} \mathbf{h} \quad (25)$$

where  $\mathbf{V}$  is the  $N \times N$  matrix with entries

$$[\mathbf{V}]_{\ell,k} = \sum_{p=1}^{M-1} \sum_{n=N-L}^N g[n-\ell]g[n-k] \cos\left(\frac{2\pi}{M}(k-\ell)p\right). \quad (26)$$

Using (25) and (23), the objective function in (12a) can be written as  $\mathbf{h}^T \mathbf{\Psi} \mathbf{h}$ , where

$$\mathbf{\Psi} = \lambda \mathbf{U} + (1 - \lambda) \mathbf{V}. \quad (27)$$

Hence, the optimization problem in (12) can be written as

$$\text{minimize } \mathbf{h}^T \mathbf{\Psi} \mathbf{h} \quad (28a)$$

$$\text{subject to } \mathbf{d}^T \mathbf{h} = 1. \quad (28b)$$

Using the classical Lagrange multiplier optimality method [21], it can be shown that the optimization problem (28) has a closed-form solution given by

$$\begin{pmatrix} \mathbf{h}_{\text{opt}} \\ \gamma \end{pmatrix} = \mathbf{A}^{-1} \mathbf{q} \quad (29)$$

where  $\gamma$  is a real scalar,  $\mathbf{q}$  is the  $(N+1)$ th column of the identity matrix of size  $(N+1)$ , and

$$\mathbf{A} = \begin{pmatrix} 2\mathbf{\Psi} & \mathbf{d} \\ \mathbf{d}^T & 0 \end{pmatrix}. \quad (30)$$

From (23), it can be seen that  $\mathbf{U}$  is symmetric positive definite, and from (25), it can be seen that  $\mathbf{V}$  is symmetric positive definite. Since  $\lambda \in [0, 1]$ ,  $\mathbf{\Psi}$  is symmetric positive definite, and therefore, it is full rank. Using this fact and the structure of  $\mathbf{A}$  given by (30), it can be shown that  $\mathbf{A}$  is also full rank and thus invertible.

REFERENCES

[1] T. Starr, J. M. Cioffi, and P. J. Silverman, *Understanding Digital Subscriber Line Technology*. Englewood Cliffs, NJ: Prentice-Hall, 1999.

[2] T. Starr, M. Sorbara, J. M. Cioffi, and P. J. Silverman, *DSL Advances*. Englewood Cliffs, NJ: Prentice-Hall, 2003.

[3] S. D. Sandberg and M. A. Tzannes, "Overlapped discrete multitone modulation for high speed copper wire communications," *IEEE J. Sel. Areas Commun.*, vol. 13, no. 9, pp. 1571–1585, Dec. 1995.

[4] G. Cherubini, E. Eleftheriou, and S. Ölçer, "Filtered multitone modulation for very high-speed digital subscriber lines," *IEEE J. Sel. Areas Commun.*, vol. 20, no. 5, pp. 1016–1028, Jun. 2002.

[5] G. Cherubini, E. Eleftheriou, S. Ölçer, and J. M. Cioffi, "Filter bank modulation techniques for very high speed digital subscriber lines," *IEEE Commun. Mag.*, vol. 38, no. 5, pp. 98–104, May 2000.

[6] S. Govardhanagiri, T. Karp, P. Heller, and T. Nguyen, "Performance analysis of multicarrier modulation systems using cosine modulated filter banks," in *Proc. Int. Conf. Acoust., Speech, Signal Processing (ICASSP)*, Phoenix, AZ, Mar. 1999, vol. 3, pp. 1405–1408.

[7] M. Hawryluck, A. Yongacoglu, and M. Kavehrad, "Efficient equalization of discrete wavelet multi-tone over twisted pair," in *Proc. Int. Zurich Seminar Broadband Communications*, Feb. 1998, pp. 185–191.

[8] B. Borna and T. N. Davidson, "Efficient design of FMT systems," *IEEE Trans. Commun.*, vol. 54, no. 5, pp. 794–797, May 2006.

[9] A. M. Tonello, "Performance limits for filtered multitone modulation in fading channels," *IEEE Trans. Wireless Commun.*, vol. 4, no. 5, pp. 2121–2135, Sep. 2005.

[10] G. Cuyppers, K. Vanbleu, G. Ysebaert, and M. Moonen, "Egress reduction by intra-symbol windowing in DMT-based transmitters," in *Proc. Int. Conf. Acoust., Speech, Signal Processing (ICASSP)*, Hong Kong, Apr. 2003, vol. 4, pp. 532–535.

[11] A. Vahlin and N. Holte, "Optimal finite duration pulses for OFDM," *IEEE Trans. Commun.*, vol. 44, no. 1, pp. 10–14, Jan. 1996.

[12] M. Pauli and P. Kuchenbecker, "On the reduction of the out-of-band radiation of OFDM-signals," in *Proc. IEEE Int. Conf. Commun.*, Atlanta, GA, Jun. 1998, vol. 3, pp. 1304–1308.

[13] Y. P. Lin and S. M. Phoong, "Window designs for DFT-based multicarrier systems," *IEEE Trans. Signal Process.*, vol. 53, no. 3, pp. 1015–1024, Mar. 2005.

[14] C. Muschallik, "Improving an OFDM reception using an adaptive Nyquist windowing," *IEEE Trans. Consum. Electron.*, vol. 42, no. 3, pp. 259–269, Aug. 1996.

[15] S. H. Muller-Weinfurtner, "Optimum Nyquist windowing in OFDM receivers," *IEEE Trans. Commun.*, vol. 49, no. 3, pp. 417–420, Mar. 2001.

[16] A. J. Redfern, "Receiver window design for multicarrier communications systems," *IEEE J. Sel. Areas Commun.*, vol. 20, no. 5, pp. 1029–1036, Jun. 2002.

[17] K. Van Acker, T. Pollet, G. Leus, and M. Moonen, "Combination of per tone equalizers and windowing in DMT-receivers," *Signal Process.*, vol. 81, pp. 1571–1579, 2001.

[18] F. J. Harris, "On the use of windows for harmonic analysis with the discrete Fourier transform," *Proc. IEEE*, vol. 66, pp. 51–83, Jan. 1978.

[19] A. V. Oppenheim and R. W. Schaffer, *Discrete-Time Signal Processing*. Englewood Cliffs, NJ: Prentice-Hall, 1989.

[20] S. K. Mitra, *Digital Signal Processing*. New York: McGraw-Hill, 1998.

[21] S. Boyd and L. Vandenberghe, *Convex Optimization*. Cambridge, U.K.: Cambridge Univ. Press, 2004.

[22] A. Tkacenko, P. P. Vaidyanathan, and T. Q. Nguyen, "On the eigenfilter design method and its applications: A tutorial," *IEEE Trans. Circuits Syst. II, Analog Digit. Signal Process.*, vol. 50, no. 9, pp. 497–517, Sep. 2003.

[23] J. G. Proakis, *Digital Communications*, 4th ed. New York: McGraw-Hill, 2001.

[24] P. J. W. Melsa, R. C. Younce, and C. E. Rohrs, "Impulse response shortening for discrete multitone transceivers," *IEEE Trans. Commun.*, vol. 44, no. 12, pp. 1662–1672, Dec. 1996.

[25] B. Farhang-Boroujeny and M. Ding, "Design methods for time-domain equalizers in DMT transceivers," *IEEE Trans. Commun.*, vol. 49, no. 3, pp. 554–562, Mar. 2001.

[26] R. K. Martin, K. Vanbleu, M. Ding, G. Ysebaert, M. Milosevic, B. L. Evans, M. Moonen, and C. R. Johnson, Jr., "Unification and evaluation of equalization structures and design algorithms for discrete multitone modulation systems," *IEEE Trans. Signal Process.*, vol. 53, no. 10, pp. 3880–3894, Oct. 2005.

[27] J. M. Cioffi, *VDSL System Requirements Document*, ANSI Contribution T1E1.4/98-043R3, Jun. 1998.



**Bahram Borna** received the B.Sc. degree in electronics engineering from Isfahan University of Technology, Iran, in 1995 and the M.Sc. degree in telecommunications engineering from the University of Tehran, Iran, in 1998. He is currently working towards the Ph.D. degree in electrical engineering at McMaster University, Hamilton, ON, Canada.

His research interests include digital signal processing techniques for communications and communications theory.



**Timothy N. Davidson** (M'96) received the B.Eng. (Hons. I) degree in electronic engineering from the University of Western Australia (UWA), Perth, Western Australia, in 1991 and the D.Phil. degree in engineering science from the University of Oxford, U.K., in 1995.

He is currently an Associate Professor in the Department of Electrical and Computer Engineering at McMaster University, Hamilton, ON, Canada, where he holds the (Tier II) Canada Research Chair in Communication Systems. His research interests are in signal processing, communications and control, with current activity focused on signal processing for digital communication systems. He has held research positions at the Communications Research Laboratory at McMaster University, the Adaptive Signal Processing Laboratory at UWA, and the Australian Telecommunications Research Institute at Curtin University of Technology, Perth, Western Australia.

Dr. Davidson was awarded the 1991 J. A. Wood Memorial Prize [for the most outstanding (UWA) graduand in the pure and applied sciences] and the 1991 Rhodes Scholarship for Western Australia. He is currently serving as an Associate Editor of the IEEE TRANSACTIONS ON SIGNAL PROCESSING and the IEEE TRANSACTIONS ON CIRCUITS AND SYSTEMS II, and as a Guest Editor for upcoming issues of the IEEE JOURNAL ON SELECTED AREAS IN COMMUNICATIONS and the IEEE JOURNAL ON SELECTED TOPICS IN SIGNAL PROCESSING.